STRUCTURAL AND OPTICAL PROPERTIES OF $Al_xIn_yGa_{1-x-y}N$ THIN FILMS

MUSLIM A. ABED

UNIVERSITI SAINS MALAYSA

2012

STRUCTURAL AND OPTICAL PROPERTIES OF $Al_xIn_yGa_{1-x-y}N$ THIN FILMS

by

MUSLIM A. ABED

Thesis submitted in fulfillment of the requirements for the degree of Doctor of Philosophy

February, 2012

ACKNOWLEDGEMENTS

First and foremost, I would like to thank Allah for granting me health and patience to finish this research. This dissertation represents a culmination of a long journey through graduate school from primary school, high school, college and the postgraduate and I am indebted to many teachers and professors for helping me reach this point.

In this Ph.D. study stage, I would like to thank my advisor, Prof. Dr. Haslan Abu Hassan for his invaluable guidance, support and trust through all these study years. Without his continuous encouragement and enduring patience, this thesis would not have been possible. Thanks again professor for having your door open every time I needed help, even though you never had the time, you always made it.

I would also like to extend my sincere thanks to the Dean of the School of Physics Prof. Dr. Zainuriah Hassan, and to Dr. Ng Sha Shiong, Dr. Sabah M. Thahab and other lecturers for their important scientific comments. Special thanks go to Dr. Michael J. Godfrey from theoretical physics group, Manchester university for his fruitful discussion with me regarding the simulation model.

I would like to thank all my dear colleague's friends for their help and encouragement. Much of this work would have been virtually impossible without the technical support offered by our helpful laboratory assistants at the School of Physics, Universiti Sains Malaysia.

Far in distance and connected in hearts, I wish to express my deepest thanks to my parents for their long time support and unconditional love. Last, and most important, I extend special thanks to my wife and my children to accompany me during this important time in our lives. Without their endless love, patience and support, I could not have a chance to complete this study.

TABLE OF CONTENTS

CHAPTER 3: FUNDAMENTAL PROPERTIES AND THEORETICAL MODELS

LIST OF TABLES

LIST OF FIGURES

LIST OF SYMBOLS

$\perp$	Direction perpendicular to *c*-axis
$\|\|$	Direction parallel to *c*-axis
a	Lattice constant
β_i	Nearest-neighbor force constant
b	Bowing parameter
c	Lattice constant
d	Distance
d_{hkl}	Interplanar spacing of the crystal planes
e^*	Effective charge
E_{loc}	Local field
E_g	Band gap energy
E	Electric field
F	Force
f_i	Oscillator strengths
h	Planck's constant
($hkil$)	Miller-Bravais indices
L	Lagrangian
M	Total effective masses for the relative coordinate
m_o	Electron mass
m^*	Effective mass
m_n	Electron effective mass
n	Number of Wigner-Seitz cells per unit volume
n_e	Number of ion pairs per unit volume
P	Polarization
q	Electron charge
R	Center-of-mass coordinate
T	Motion energy
u	Displacement of the ion
V	Potential energy
ω_L	Longitudinal optical phonon frequency
ω_T	Transverse optical phonon frequency
α	Absorption coefficient
ε_∞	High optical dielectric constant
ε_o	Static dielectric constant
ε_0	Permittivity of vacuum
ε_r	Relative dielectric constant
γ	Electronic polarizability
ν	Frequency
θ	Incident / Diffraction angle
2θ- w	2 theta-omega scan mode for XRD measurements
μ	Reduce masses
∞	Infinity
ω	Photon frequency
λ	Wavelength
λ_{Abs}	Absorption edge

LIST OF MAJOR ABBREVIATIONS

2D	Two dimensional
3D	Three dimensional
AFM	Atomic force microscope
ACF	Alloy compositional fluctuations
AlN	Aluminum nitride
AlInN	Aluminum indium nitride
AlGaN	Aluminum gallium nitride
AlInGaN	Aluminum indium gallium nitride
a.u.	Arbitrary unit
BZ	Brillouin zone
CB	Condition band
CCFL	Cold cathode fluorescent lamps
CRT	Cathode-ray tube
CL	Cathodoluminescence
CD	Compact disk
DVD	Digital video disk
EDX	Energy dispersive X-ray
EHPs	Electron hole pairs
eV	Electron volt
e-beam	Electron beam
FTIR	Fourier transform infrared
FWHM	Full width at half maximum
HR	High resolution
HVPE	Hydride vapor phase epitaxy
IR	Infrared
InN	Indium nitride
InGaN	Indium gallium nitride
I-V	Current-voltage
LD	Laser diode
LED	Light emitting diode
LO	Longitudinal optical
M	Metal
MBE	Molecular beam epitaxial
MOCVD	Metalorganic chemical vapour deposition
NBE	Near band edge
NA	Not available
NRCs	Nonradiative recombination centers
PA	Plasma-assisted
PBN	Pyrolytic boron nitride
PL	Photoluminscence
PA-MOCVD	Plasma assisted MOCVD
PUC	Pseudo unite cell
PMT	Photomultiplier tube
QWs	Quantum wells
RC	Rocking curve
RF	Radio frequency

ROM	Read only memory
RHEED	Reflection high energy electron diffraction
RMS	Root mean square
SEM	Scanning electron microscope
SC	Semiconductor
SIS	Surface imaging systems
TEM	Transmission electron microscopy
TO	Transverse optical
TD	Threading dislocations
UHV	Ultra high vacuum
UV-VIS	Ultraviolet-visible spectroscopy
UV	Ultraviolet
VB	Valence band
VIS	Visible
XRD	X-ray diffraction
YL	Yellow luminescence

CIRI STRUKTUR DAN OPTIK BAGI FILEM NIPIS $Al_xIn_yGa_{1-x-y}N$

ABSTRAK

Kajian tertumpu kepada penyelidikan sifat struktur dan optik bagi tiga set saput tipis nitrida. Set pertama ialah nitrida ternari $In_xGa_{1-x}N$ ($0.2 \leq x \leq 0.8$), sementara dua set yang lain ialah nitrida kuaternari $Al_xIn_yGa_{1-x-y}N$, set yang pertama dengan Al malar, $x = 0.06$, dan In dalam julat $0 \leq y \leq 0.10$, dan set yang kedua dengan In malar, $y = 0.10$, dan komposisi Al yang berubah dalam julat $0 \leq x \leq 0.20$. Kajian juga merangkumi penyelidikan mod fonon optik berpusat zon, terutamanya mod A_1(LO), E_1(TO), E_2(Rendah) dan E_2(Tinggi) bagi bahan nitrida ternari dan kuaternari secara teori menggunakan model sel unit pseudo (PUC) dan secara eksperimen menggunakan spektroskopi Raman dan FTIR.

Saput ternari dan kuaternari ditumbuhkan di atas satah-*c* (0001) substrat nilam dengan lapisan penimbal AlN menggunakan teknik epitaksi alur molekul dibantu plasma (PA-MBE). Sifat struktur dan optik semikonduktor nitrida ternari dan kuaternari diselidiki menggunakan peralatan tak sentuhan dan tak memusnahkan, yang merangkumi pencirian struktur seperti mikroskop imbasan elektron (SEM), sebaran tenaga sinar-X (EDX), mikroskop daya atom (AFM) dan belauan sinar-X resolusi tinggi (HR-XRD), sementara pencirian optik merangkumi teknik pantulan spektra, spektroskopi ultraungu-nampak (UV-VIS), spektroskopi fotoluminesens (PL), spektroskopi Raman dan spektroskopi pantulan inframerah (IR) terkutub.

Pertama, kajian awal telah dilaksanakan tentang sifat struktur dan optik nitrida ternari $In_xGa_{1-x}N$. Keputusan menunjukkan bahawa saput ditumbuhkan tanpa sebarang pemisahan fasa dan mempunyai struktur wurtzit dengan kualiti habluran yang tinggi. Pengukuran optik pula mendedahkan pengurangan keamatan bersepadu

puncak utama dan kedudukan puncak dianjak ke kawasan bertenaga rendah (anjakan merah) apabila kandungan komposisi In ditingkatkan.

Kedua, sifat struktur dan optik semikonduktor nitrida kuaternari $Al_xIn_yGa_{1-x-y}N$ dengan Al malar telah dikaji. Pengukuran XRD mengesahkan aloi $Al_xIn_yGa_{1-x-y}N$ mempunyai struktur wurtzit dan ditumbuhkan tanpa sebarang pemisahan fasa. Imej SEM dengan analisis komposisi unsur oleh EDX menghasilkan bukti yang menunjukkan kehadiran kecacatan di dalam sampel yang menyebabkan pengurangan kualiti sampel. Sifat optik menunjukkan pengurangan keamatan bersepadu dan peningkatan anjakan merah dengan peningkatan kandungan In.

Ketiga, sifat struktur dan optik semikonduktor nitrida kuaternari $Al_xIn_yGa_{1-x-y}N$ dengan In malar telah dikaji. Pengukuran struktur menunjukkan saput ditumbuh tanpa sebarang pemisahan fasa dan mempunyai struktur wurtzit dengan kualiti habluran yang tinggi. Pengukuran optik mempamerkan peningkatan keamatan bersepadu puncak utama dan kedudukan puncak dianjak ke kawasan tenaga tinggi dengan peningkatan kandungan Al.

Akhir sekali, keputusan teori PUC dibandingkan dengan keputusan eksperimen bagi semua bahan nitrida ternari dan kuaternari, yang mana fonon aktif optik membujur bagi AlGaN dan InGaN menunjukkan kelakuan satu-mod. Sementara bagi AlInN dan kuaternari AlInGaN, fonon optik membujur mempamerkan kelakuan dua-mod. Ramalan teori adalah bersetuju dengan keputusan eksperimen. Frekuensi E_1(TO) dan E_2(Tinggi) telah diperolehi daripada sampel nitrida kuaternari, yang keputusannya belum pernah diterbit atau dikaji di mana-mana.

STRUCTURAL AND OPTICAL PROPERTIES OF $Al_xIn_yGa_{1-x-y}N$ THIN FILMS

ABSTRACT

The studies focus on the investigations of the structural and optical properties of three sets of nitride thin films. The first set is $In_xGa_{1-x}N$ ($0.2 \leq x \leq 0.8$) ternary nitride, the other two sets are $Al_xIn_yGa_{1-x-y}N$ quaternary nitrides, the first one with constant Al, $x = 0.06$, and In in the range of $0 \leq y \leq 0.10$, while the second set is with constant In, $y = 0.10$, and variable Al composition ranging from $0 \leq x \leq 0.20$. As well as the study of the zone-center optical phonon modes, especially the A_1(LO), E_1(TO), E_2(Low) and E_2(High) modes for ternary and quaternary nitride materials theoretically using pseudo unit cell (PUC) model and experimentally using Raman and FTIR spectroscopy.

The ternary and quaternary films were grown on *c*-plane (0001) sapphire substrates with AlN as buffer layers using plasma assisted molecular beam epitaxy (PA-MBE) technique. The structural and optical properties of the ternary and quaternary nitride semiconductors have been investigated by several non-contact and non-destructive equipments, which include structural characterizations such as scanning electron microscopy (SEM), energy dispersive X-ray (EDX), atomic force microscopy (AFM) and high resolution X-ray diffraction (HR-XRD), while the optical characterizations include, spectral reflectance technique, ultraviolet-visible (UV-VIS) spectroscopy, photoluminescence (PL) spectroscopy, Raman spectroscopy and polarized infrared (IR) reflectance spectroscopy.

Firstly, initial works on the structural and optical properties of ternary $In_xGa_{1-x}N$ nitrides have been studied. The results showed that the films are grown without any phase separation and have a wurtzite structure with high crystalline

quality. While the optical measurements revealed a reduction of the dominant peak integrated intensity and the peak position shifts to the low energy region (red shift) as the amount of In composition is increased.

Secondly, the structural and optical properties of quaternary $Al_xIn_yGa_{1-x-y}N$ nitride semiconductors with constant Al have been studied. The XRD measurements confirmed that the $Al_xIn_yGa_{1-x-y}N$ alloys had wurtzite structure and grown without any phase separation. SEM images with element composition analysis by EDX provided the evidence to show the existence of defects inside the samples which caused a decreased in the quality of the samples. Optical properties showed reduction of the integrated intensity and an increasing red shift with increasing In content.

Thirdly, the structural and optical properties of quaternary $Al_xIn_yGa_{1-x-y}N$ nitride semiconductors with constant In have been investigated. The structural measurements indicated that the films are grown without any phase separation and have a wurtzite structure with high crystalline quality. The optical measurements exhibited an enhancement of the dominant peak integrated intensity and the peak position shifts to the high energy region with increasing Al content.

Lastly, the theoretical PUC results were compared with experimental results for all ternary and quaternary nitride materials, of which the active longitudinal optical phonons of AlGaN and InGaN reveal a one-mode behavior. While for the AlInN and quaternary AlInGaN the longitudinal optical phonons exhibit a two-mode behavior. The theoretical predictions are in agreement with the experimental results. Finally, frequencies of the E_1(TO) and E_2(High) for our quaternary nitride samples have been obtained, which have not been published or studied elsewhere.

CHAPTER 1

INTRODUCTION

1.1 Introduction to III-V nitrides

The III-V semiconductors have traditionally been divided into two parts. The first one is the conventional III-Vs which include, arsenides, phosphides and antimonides while the second one is the nitrides which are treated separately due to differences in growth conditions, crystal structure and miscibility.

The conventional III-Vs have a relatively smaller band gap than the nitrides, which lend them useful for light-emitting applications with limited wave length that starts from green to infrared and in high-speed electronic switching applications. These semiconductors are easily broken, chemically altered and etched. Also, the conventional III-Vs are chemically and structurally less stable than the III-nitrides making them not suitable for high temperature and corrosive environments. Our research works will be focused on the III-Nitrides semiconductors**.** The group III-nitride compounds have attracted considerable interest due to their applications for optoelectronic devices, which are active in the blue and ultraviolet spectral regions with high quantum efficiency (Hirayama et al., 2002a; Marinelli et al., 2001; Piner et al., 1996; Zhang et al., 2000). In particular, their binaries (AlN, GaN, and InN), ternaries ($In_xGa_{1-x}N$, $Al_xGa_{1-x}N$, and $Al_xIn_{1-x}N$) and quaternaries $Al_xIn_yGa_{1-x-y}N$ in wurtzite structure having direct band gaps, covering a broad spectral range from infrared to deep UV (0.7 eV for InN up to 6.2 eV for AlN) (Davydov et al., 2002a; Madelung, 1991) as shown in Fig. 1.1. Direct band gap nitrides semiconductors can easily produce photons by the recombination of an electron in the conduction band with a hole in the valence band.

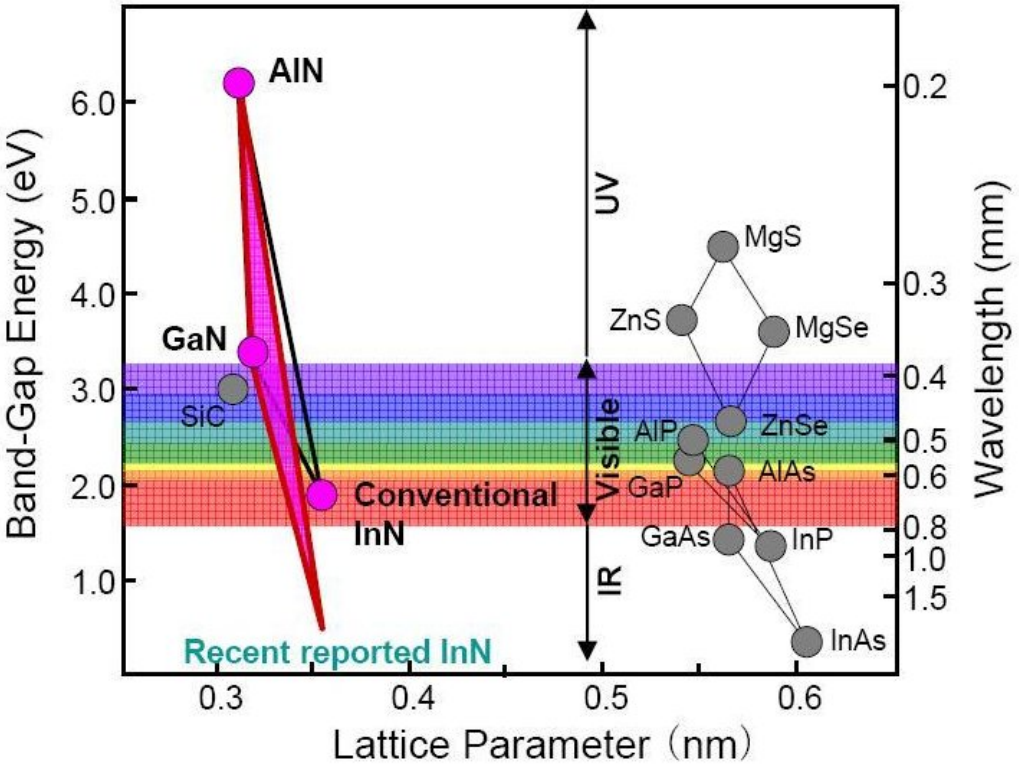

Figure 1.1: Lattice parameter versus band gap and wavelength of binary nitride in comparison with other semiconductors, e.g. ZnS, MgS. (Adapted from Christian, 2010)

It has been shown that group-III nitrides represent the ideal material system for optoelectronic applications, such as blue and green light-emitting diodes, laser-diodes, high-temperature and high-power electronics devices (Nakamura & Fasol, 1997; Pearton et al., 2000). These many encouraging applications of GaN and their alloys are, however, restricted by problems in their epitaxial growth. The problems include:-

1.1.1. Substrates for epitaxy

The major problem that has delayed the group III-nitride thin films research is the lack of a native substrates, which include GaN, AlN, and their alloys. The growth of a semiconductor on a substrate of the same material is called homoepitaxy

which lead to high quality films due to near lattice matching. Nitrides thin films growth on foreign (non-native) substrates is known as heteroepitaxy.

Sapphire is a foreign substrate which has been the most popular choice in group III-V nitride but not the best choice in terms of lattice mismatch (a +33% lattice mismatch which is reduced to 16% by in-plane rotation of 30° around the *c*-axis of GaN) as shown in Figure 1.2 (a) and (b). Additionally, sapphire is an electrical insulator, such that mesa-etching is necessary for electrical contacts which make device fabrication more difficult, besides. The poor thermal conductivity of sapphire seriously impedes its use for high power devices, but it has the advantage which includes, hexagonal symmetry, easy for handling and pre-growth cleaning, availability of large area, high-quality crystals, its transparent nature and high temperature stability (~ 1000 °C) which is required for epitaxial growth of III-nitrides.

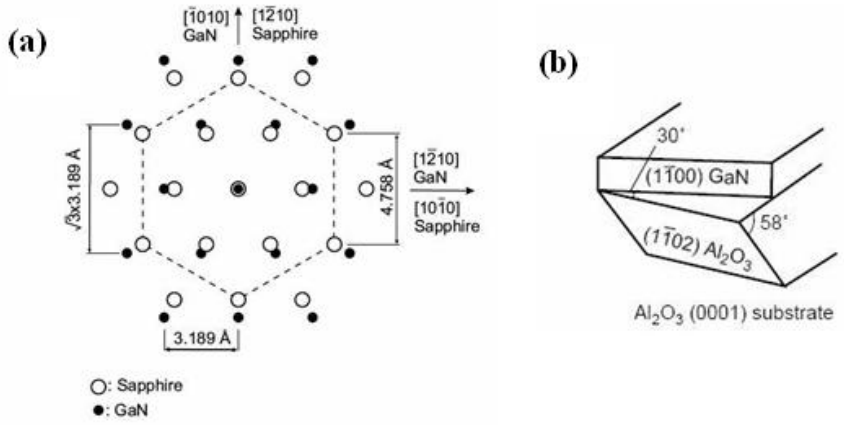

Figure 1.2: (a) Schematic illustration of the lattice mismatch for GaN grown onto an Al_2O_3 (0001) sapphire substrate (Nakamura & Fasol, 1997), (b) rotation of the GaN onto sapphire substrate (Kuramata, Horino, & Domen, 1998)

Due to the large thermal expansion mismatch and the lattice mismatch between sapphire and nitrides, the grown epitaxial layer will be strained. There are

two types of strains in heteroepitaxy growth of semiconductor. The first one appear if the epitaxial layer lattice constant is smaller than the substrate lattice constant. The epitaxial layer will become under tensile strain. The second, if the epitaxial layer has a larger lattice constant than the substrate, the epitaxial layer will experience a compressive strain. These two kinds of strains will change the electrical and optical properties of the nitrides semiconductor with respect to their original properties.

1.1.2 Strong polarization

Another peculiarity in the wurtzite III-nitride semiconductors is that they do not have the inversion symmetry along the crystal *c*-axis [0001] direction, because of the difference in metal-nitrogen atoms size and the bonding force between metal-nitrogen atoms is not equivalent. Therefore, the center of the negative charges and the center of the positive charges are not located at the same position. This fact results in a strong macroscopic polarization along the *c*-axis [0001] direction. Since this polarization effect occurs in the equilibrium lattice of III- nitrides at zero strain, it is called spontaneous polarization (Bernardini, Fiorentini, & Vanderbilt, 1997). While the piezoelectric polarization is caused by strain, which is formed as layers are grown on lattice mismatched substrate, which it physically derives from the spatial separation of the electron and hole wave functions that occur when strain is applied to a crystal, thus, the movement of the charges (electron and hole) will produce an electric field. Consequently, the poor electron-hole overlap due to large electric fields reduce the radiative recombination and cause red-shifting of the photoluminescence peak and decreasing the peak intensity for the devices (Bernardini & Fiorentini, 1998; Deguchi et al., 1999). The total polarization charges are the sum of the charges

contributed to spontaneous polarization and charges generated from piezoelectric polarization.

1.1.3 Indium segregation

There is another potential obstacle for III-nitrides semiconductors called the indium segregation phenomenon. This occurs because the InN and GaN are not completely soluble in each other, even at the highest thin film growth temperature which is approximately 800 ºC (Ho & Stringfellow, 1996). This phenomenon is more pronounced in alloys with higher amounts of the In/Ga ratio.

Moon et al. (Moon et al., 2001) found that In segregation can take two forms. The first, surface segregation forms as self assembled quantum dot of In that acts to enhance the radiative recombination center. The second is regions formed in the InGaN film during the higher temperature growth for the capping layers of the device, thus. These regions tend to act on the active region of the emitter very inhomogeneously which results in very broad emission bands and can introduce high concentrations of non-radiative recombination centers which yield poor optical properties of the devices.

1.1.4 Doping of III-Nitrides

Doping of III-nitrides semiconductors has proven to be another big challenge faced by the nitride research technology. It is well known that the most common n-type dopant for GaN is silicon (Si) while the most popular choice for p-type dopant is magnesium (Mg).

Our study deals with undoped samples (unintentionally doped, which are usually found to be n-type in the low 10^{16} cm^{-3} concentration range). Therefore, we will attempt to discuss a simple idea on this problem without revealing more details

on it. P-type doping is clearly the more difficult side of this problem. There are several reasons for the difficulty of p-type doping in GaN and their alloys, first being the lack of dopants, which form shallow acceptor levels. Currently, the high activation energy level of Mg acceptors, which is fairly deep (160-210 meV) from the valence band edge, forces an increase in the Mg density close to its solubility limit, which makes the free hole concentration obtained remains very small (Tanaka et al., 1994). Additionally, this low hole concentration leads to a high resistivity, low mobility and short minority carrier diffusion length in p-type layers in devices.

The second, many GaN films, particularly ones of lower quality, tend to have a high ($n > 10^{17}$ cm^{-3}) background n-type concentration. Compared with GaN, InGaN has been shown to possess higher background donor concentrations, these donors compensate intentionally added acceptors, thus, these carriers must be fully compensated before p-type character can be achieved. As a result, at a room-temperature, in AlGaN alloys, the hole concentration that can be achieved with Mg doping has been observed to decrease rapidly with increasing Al content (Katsuragawa et al., 1998; Suzuki et al., 1998) because the depth of the Mg acceptor level goes deeper fast with the addition of Al in the AlGaN alloy (Tanaka et al., 1994).

The use of quaternary nitrides provide some solutions to the problems mentioned above, because the use of quaternary nitrides $Al_xIn_yGa_{1-x-y}N$ alloys should allow almost independent control of the lattice constant and energy band gap by varying the indium (In) and aluminum (Al) compositions (Monroy et al., 2003). On the other hand, the strain engineering for III-nitrides based semiconductor is also a controversial issue. For InGaN quantum wells (QWs), the InGaN wells are always subjected to compressive strains while the AlGaN QWs always under tensile strain.

Thus, the strain condition of quaternary AlInGaN (under tensile, compressive and zero strains) depends on the content of aluminum and indium mole fractions (Aumer et al., 2001; Khan et al., 2000; McIntosh et al., 1996).

The high efficiency of InGaN-based LEDs is generally attributed to a strong In-induced exciton localization that prevents carriers to reach nonradiative recombination centers (NRCs) (Nakamura, 1998; Chichibu et al., 2006). On the contrary, the use of ternary AlGaN (UV-LEDs) shows a much lower efficiency than InGaN-LEDs due to difficulties to achieve p-type conductivity with increasing Al content and to the lack of efficient exciton localization, which makes carriers very sensitive to NRCs. Therefore, Hirayama et al. (Hirayama et al., 2002a) proposed that the use of In-segregation effect (surface segregation forms) in the quaternary AlInGaN alloys for obtaining strong UV emission at room temperature (RT) and found that the emission is greatly improved in comparison with that of GaN, InGaN or AlGaN based QWs. Thus we believe that quaternary AlInGaN layers with stronger spatial potential fluctuations would be the ideal candidate for UV LEDs application as the active region for these devices which has several advantages, including a strong spontaneous emission due to an enhanced radiative recombination of localized excitons/carrier's at band-tail states, and a better lattice match to AlN resulting in a decrease of dislocations (Ryu et al., 2002; Hashemizadeh et al., 2005; Onuma et al., 2006; Song et al., 2003).

With respect to the spontaneous and piezoelectric polarizations which play an important role as discussed in section 1.1.2, the use of the quaternary layers may enhance the capability for investigating the effect of polarization-induced field/charge in quantum wells heterostructure. However, in spite of these advantages, not many works have addressed the growth of quaternary layers by PA-MBE (Lima

et al., 2000; Iwata et al., 2003; Monroy et al., 2003a; Dimakis et al., 2003; Wang et al., 2007) because the growth of high quality AlInGaN layers require a balance between the high temperatures suited for Al containing layers and the low temperatures necessary for incorporation of In. Hence, high quality quaternary AlInGaN materials exhibit interesting features as their emission intensities can be higher than the ternary AlGaN and InGaN alloys for certain Al and In compositions (Chen et al., 2002).

We will focus to investigate the fundamental properties of ternary InGaN and quaternary AlInGaN nitrides semiconductors materials by studying the structural and optical characterizations such as the surface morphology, lattice constant, an optical band gap, the band gap bowing parameter as well as the behavior of the optical phonon mode theoretically and experimentally. The phonon modes behavior of quaternary nitrides have not been widely investigated experimentally, due to the lack of samples covering the whole composition of the quaternary, besides that the quaternary nitrides are very complex materials and cannot be explained by the usual properties of wurtzite structure. Thus we will try to investigate the phonon properties of the ternary and quaternary samples using Raman and FTIR spectroscopy measurements and compare the results with theoretical model of lattice vibrations using a pseudo unit cell (PUC) model. On the other hand, the phonons mode results of quaternary samples remain incomplete experimentally to date and there has been no agreement, whether to consider the $Al_xIn_yGa_{1-x-y}N$ having one-mode, two-mode or mix-mode behavior. Thus, this experimental study and its comparison with theoretical study by using PUC model will provide some answers for this issue.

1.2 Objectives of this research

The aim of this research is to investigate the material quality, surface morphology, surface roughness, lattice constant *c*, an energy band gap, the band gap bowing parameter, and the behaviors of the optical phonon modes in the Brillouin zone (BZ), especially the A_1(LO), E_1(TO), E_2(Low) and E_2(High) modes by studying the effects of changing the alloys composition, by varying *x* and *y* on the structural and optical properties of ternary ($In_xGa_{1-x}N$, $Al_xGa_{1-x}N$, or $Al_xIn_{1-x}N$) and quaternary ($Al_xIn_yGa_{1-x-y}N$) III-nitride semiconductors. The ternary and quaternary films were grown on *c*-plane (0001) sapphire substrates with AlN as buffer layers using plasma assisted molecular beam epitaxy (PA-MBE) technique. The specific objectives of the research include:

1. Study the effects of the increase in indium In mole fraction on the structural and optical properties of ternary $In_xGa_{1-x}N$ nitride semiconductors.
2. Study the effects of the increase in indium In mole fraction with constant aluminum Al = 0.06 on the structural and optical properties of quaternary $Al_xIn_yGa_{1-x-y}N$ nitride semiconductor samples.
3. Evaluate the effects of the increase in aluminum Al mole fraction with constant indium In = 0.1 on the structural and optical properties of quaternary $Al_xIn_yGa_{1-x-y}N$ nitride semiconductors.
4. Build a theoretical model using visual Fortran language programming to study the phonon frequency, phonon mode and dielectric constants for the ternary and quaternary III-nitride semiconductor and compare the results with Raman and FTIR spectroscopy experimental results.

The structural and optical properties of ternary and quaternary nitride semiconductors have been carried out by several non-contact and non-destructive

equipments, which include structural characterizations such as scanning electron microscopy (SEM), energy dispersive X-ray (EDX), atomic force microscopy (AFM) and high resolution X-ray diffraction (HR-XRD), while the optical characterizations include, spectral reflectance technique, ultraviolet-visible (UV-VIS) spectroscopy, photoluminescence (PL) spectroscopy, Raman spectroscopy and polarized infrared (IR) reflectance spectroscopy.

In general, this work provides a better understanding on the fundamental properties of the wide band gap ternary and quaternary nitrides semiconductor materials.

1.3 Originality of the research works

A number of original works have been carried out in this research work, which lies in the experimental and theoretical investigations by means of the studies of the influences and the change in alloy composition x for the ternary and x, y for the quaternary III- nitrides semiconductors.

For instance, the experimental investigations cover the structural and optical properties of three sets of nitrides, first one is ternary and the other two sets are quaternary nitrides, with all these three sets studied for the first time within the same composition range and in the same thickness by plasma assistance molecular beam epitaxy.

The details of these three sets include, first set $In_xGa_{1-x}N$ ternary nitrides with In composition x ranged from 0.2 to 0.8, the second set $Al_xIn_yGa_{1-x-y}N$ quaternary nitrides semiconductors with constant Al and In composition ranged from 0.01 to 0.1, the third set is the same quaternary nitrides but in a reverse manner i.e., constant In and varied Al composition ranged from 0.1 to 0.2.

On the other hand, the theoretical studies used a visual Fortran language programming to build a PUC model for ternary and quaternary nitrides to simulate and investigate the phonon frequency, phonon modes, and dielectric constants for all these samples. The calculation for each study was performed twice which its quite new and not mentioned anywhere else, first using $E_1(LO)/E_1(TO)$ with the dielectric constants perpendicular to the *c* axis and a second time using $A_1(LO)/A_1(TO)$ with the dielectric constants parallel to the *c* axis, to get the $E_1(TO)$ and $A_1(LO)$ modes, respectively. Besides that we calculated the phonon frequency in terms of wave number (cm^{-1}) instead of energy (meV) for easy comparison with our experimental results (Raman and FTIR) which are quoted in the terms of the wave number (cm^{-1}).

1.4 Outline of the thesis

The experimental and theoretical works presented in this dissertation is organized as follows:-

Chapter 2 introduces an overview of the wurtzite III-nitrides which include, binary (GaN, AlN, and InN), ternary ($Al_xGa_{1-x}N$, $In_xGa_{1-x}N$ and $Al_xIn_{1-x}N$) and quaternary ($Al_xIn_yGa_{1-x-y}N$) materials are given. However, this chapter describes the nitride early studies such as epitaxial growth techniques, band gap energy bowing parameter and the behavior of the Brillouin zone (BZ) optical phonon modes.

Chapter 3 reports on the fundamental properties of the ternary and quaternary nitrides, such as the crystalline structure, lattice constant and energy band gap bowing parameter, besides the behavior of the optical phonon mode in the BZ. Also the theoretical PUC model for the ternary and quaternary nitrides is presented, which generally include the details on the phonon frequency, dielectric constants and oscillator strengths.

In Chapter 4, the basic principles of the characterization tools, process equipments, and materials are discussed. These include the experimental details for each instrumental setup, the operating conditions as well as the resolution, and the sample details.

Chapter 5 focuses on the results and discussion of the ternary nitride semiconductors $In_xGa_{1-x}N$ ($0.2 \leq x \leq 0.8$), which consists of the structural properties such as SEM, EDX, AFM and HR-XRD and optical properties such as films thickness, UV-VIS and PL measurements. The same format is repeated in the next two chapters but the difference is that the quaternary nitride is used instead of the ternary $In_xGa_{1-x}N$. Hence Chapter 6 deals with the quaternary nitrides semiconductor ($Al_xIn_yGa_{1-x-y}N$) with constant aluminum $x = 0.06$ and indium range from ($0 \leq y \leq 0.10$), while Chapter 7 deals with the quaternary nitrides semiconductor ($Al_xIn_yGa_{1-x-y}N$) with constant indium $y = 0.10$ and aluminum range from ($0 \leq x \leq 0.20$).

Chapter 8 contains a comparison between Raman and FTIR experimental measurements with the PUC theoretical model for ternary and quaternary nitrides materials.

In the final Chapter 9, the conclusion of the thesis with a summary of the research work is presented. A few recommendations for future researches are also included.

CHAPTER 2

LITERATURE REVIEW

2.1 Introduction

Group III-nitrides of GaN, AlN and InN and their alloys can crystallize in three crystal structures: the wurtzite (WZ), zinc blende (ZB), and rock salt. Under ambient conditions, the thermodynamically, chemically and structurally stable structure is wurtzite for bulk AlN, GaN, and InN due to the strong ionic bond between a group III atoms and nitrogen atoms. The wurtzite structures are all direct band gaps. The zinc blende structure for GaN and InN is metastable and has been stabilized by epitaxial growth on substrate reflecting structural compatibility likes GaAs. Also, unlike the wurtzite form, the zinc-blende form of AlN does not have a direct band gap. A phase transition to the rock salt form structure takes place at high pressure. Thus, the present work is solely confined and mainly concerned with the wurtzite III-nitride material structure which had provided the best result for optoelectronic technical application. Therefore, in this chapter the overview of the wurtzite binary, ternary, and quaternary nitrides will be discussed briefly. The review will be focusing on the band gap energy as well as the bowing parameter and the behavior of the optical phonon modes.

2.2 Overview on the binary compound semiconductor

As mentioned earlier, GaN and its related alloys have attracted much attention due to their important optoelectronic applications in the blue to UV range as well as in the area of high temperature, high frequency, and high power electronics devices. A full understanding of the ternary AlGaN, InGaN and AlInN alloy system

could not be achieved before the binary GaN, AIN and InN materials are well understood. Thus, the following sections will discuss the wurtzite binary compounds semiconductors.

2.2.1 Wurtzite GaN

GaN was first synthesized by Fischer and Schroter in 1910 (Fischer & Schroter, 1910), follow by Johnson and co-workers in the 1932 by passing ammonia (NH_3) gas over hot liquid gallium (Ga) at elevated temperatures (900 °C-1000 °C) (Johnson, Parsons, & Crew, 1932). This method resulted in a powder consisting of small needles and platelets of GaN. Maruska and Tietjen then grew the first GaN single crystal on a sapphire substrate by hydride vapor phase epitaxy (HVPE) in 1969 (Maruska & Tietjen, 1969). The research continues by many research groups until now to get GaN with high crystal quality.

The first major improvement in the GaN material quality was achieved by the development of nucleation layer in 1983 by Yoshida et al. (Yoshida, Misawa, & Gonda, 1983a). Using the MBE technique with sapphire substrates, they demonstrated that the quality of the GaN was improved significantly by first growing an AlN nucleation layer. After that, Amano et al. (Amano et al., 1986) and Nakamura (Nakamura, 1991) found that it is necessary to grow thin layers of A1N or GaN (as buffer layer) at low temperatures (~ 500 °C) in between the sapphire and the main layer. This buffer layer greatly reduced the native defect concentration by reducing the effects of the lattice mismatch which yielded the lowest dislocation density resulting in good crystal and optical quality material (Akasaki et al., 1989).

GaN is a direct band gap semiconductor, with a wide band gap of 3.4 eV, with lattice constants a = 3.189 Å, c = 5.185 Å (Vurgaftman & Meyer, 2003; Vurgaftman, Meyer, & Ram-Mohan, 2001).

With respect to the behavior of the optical phonon modes, the first-order Raman scattering is caused by phonons with wave vector $k \approx 0$ because of a momentum conservation rule in the light scattering process. The wurtzite structure of GaN and their alloy has four atoms per unit cell (Loudon, 1964) which the group theory predicts eight sets of phonon normal modes at the BZ: $2A_1 + 2E_1 + 2B_1 + 2E_2$. Among them, one set of A_1 and E_1 modes are acoustic, while the remaining six modes, $A_1 + E_1 + 2B_1 + 2E_2$ are optical. In our study, we are only concern on the optical phonon modes, in which the A_1 and B_1 modes give atomic displacements along the *c*-axis, while the others, E_1 and E_2, give atomic displacements perpendicular to the *c*-axis. Here, the A_1 and E_1 modes are both Raman and infrared (IR) active (i.e., they are polar modes), while the two E_2 modes are only Raman active (i.e., nonpolar modes), and the two B_1 modes are neither Raman nor IR active (silent modes) (Cardona & G¨untherodt, 1982; Tinkham, 1964). The frequency of an optical phonon which is infrared active is split into a longitudinal (LO) and a transverse (TO) component by the macroscopic electric field associated with the relative atomic displacement of the longitudinal phonons. This electric field serves to stiffen the force constant of the phonon and thereby raise the frequency of the (LO) over that of the (TO) (Bergman et al., 1999). More details of the optical phonon mode and its behavior regarding a one-mode, a two-mode or a mixed mode will be given in Chapter 3.

The wide spread studies of the zone-center optical phonons in GaN material has led to some uncertainty in the phonon frequencies, especially of the optical phonon modes. The theoretical and experimental phonon frequencies for GaN found in this literature review are listed in Table 2.1.

Table 2.1: Phonon modes in wurtzite GaN

Phonon modes	**Experimental (cm^{-1})**	**Theoretical (cm^{-1})**
E_2 (low)	143–146[a], 144[c], 144[b], 145[h]	142[g], 153[c], 143[d], 137[e], 146[f]
E_2 (high)	560–579[a], 567.6[c], 569[b], 567[h]	576[g], 565[c], 579[d], 592[e], 560[f]
E_1(LO)	741–741[a], 741[c], 743[b], 742[h]	757[g], 739[c], 757[d], 741[e], ---
E_1(TO)	556–559[a], 558.8[c], 561[b], 561[h]	568[g], 554[c], 568[d], 555[e], 556[f]
A_1(LO)	710–735[a], 734[c], 735[b], 735[h]	748[g], 734[c], 748[d], 732[e],---
A_1(TO)	533–534[a], 531.8[c], 533[b], 533[h]	540[g], 546[c], 541[d], 546[e], 534[f]

[a] Taken from (Akasaki & Amano, 1994);
[b] Taken from (Azuhata et al., 1995);
[c] Taken from (Davydov et al., 1998);
[d] Taken from (Karch, Wagner, & Bechstedt, 1998);
[e] Taken from (Tütüncü, Srivastava, & Duman, 2002);
[f] Taken from (Miwa & Fukumoto, 1993);
[g] Taken from (Wagner & Bechstedt, 2002);
[h] Taken from (McNeil, Grimsditch, & French, 1993).

2.2.2 Wurtzite AlN

The first synthesis of AlN was realized by Fichter in 1907 (Fichter, 1907). Slack and McNelly (Slack & McNelly, 1976) suggested a technique to produce high quality AlN powder from the Al metal using AlF_3 as an intermediate product. The AlN powder can be converted to a single crystal by sublimation method in a closed tungsten crucible or in an open tube with a nitrogen gas flow. Also AlN powder can be produced by nitridation of Al metal powder or by the reduction of alumina with admixed fine carbon particles in the presence of nitrogen or ammonia (Huseby, 1983).

The hexagonal aluminum nitride has an ultra-wide direct band gap ($E_{g,\mathrm{dir}}$ = 6.28 eV) among the III-N compounds. Besides it has a high melting point (3000 °C), high thermal conductivity (2.6 W/cm.K), high thermal stability, large dielectric constant, high hardness, and an excellent electrical insulator. These properties are both physically interesting and technologically important (Jain et al., 2000; Shiosaki et al., 1980). Furthermore, the most widely accepted lattice constants

of the crystal structure of wurtzite AlN is a = 3.112 Å, c = 4.982 Å (Vurgaftman, Meyer, & Ram-Mohan, 2001).

AlN has the potential for significant applications in the microelectronic and optical device which is especially useful for high power applications due to its enhanced thermal conductivity. In addition, AlN is used as a buffer layer in the growth of multiple quantum well structures and in a highly efficient superlattice cladding layer (Ohba & Yoshida, 1998; Schenk et al., 2001).

The first-order phonon frequencies for hexagonal AlN have been intensively studied too. Typical phonon frequencies observed using Raman scattering and polarized infrared (IR) reflectance spectroscopies as well as theoretically studies from the literatures are listed in Table 2.2.

Table 2.2: Phonon modes in wurtzite AlN

Phonon modes	**Experimental (cm^{-1})**	**Theoretical (cm^{-1})**
E_2 (low)	246.1[a], 246[b], 248.6[c], 247.5[d], 252[e]	241[d], 252[f], 237[g]
E_2 (high)	655.1[a], 655[b], 657.4[c], 655.5[d], 660[e]	667[d], 667[f], 667[g]
E_1(LO)	909.6[a], ---, 912[c], 910.1[d], 916[e]	924[d], 922[f], 919[g]
E_1(TO)	667.2[a], 668[b], 670.8[c], 669.3[d], 673[e]	677[d], 673[f], 677[g]
A_1(LO)	888.9[a], 890[b], 890[c], 891[d], 893[e]	898[d], 881[f], 893[g]
A_1(TO)	608.5[a], 608[b], 611[c], 608.5[d], 614[e]	618[d], 615[f], 619[g]

[a] Taken from (Tischler & Freitas, 2004);
[b] Taken from (Bergman et al., 1999b);
[c] Taken from (Davydov et al., 1998);
[d] Taken from (Haboeck et al., 2003);
[e] Taken from (Hayashi et al., 1991);
[f] Taken from (Karch, Wagner, & Bechstedt, 1998);
[g] Taken from (McNeil, Grimsditch, & French, 1993).

2.2.3 Wurtzite InN

Juza and Hahn in1938 (Juza & Hahn, 1938) obtained synthesized powder of InN from decomposition of $InF_6(NH_4)_3$ at 600 °C. They determine the crystallographic properties of this material by X-ray diffraction and reported the

crystal structure of wurtzite InN having lattice parameters a = 3.5377 Å, c = 5.7037 Å, which are in excellent agreement with the present reported values of a = 3.54 Å, c = 5.70 Å (Harima, 2002; Vurgaftman & Meyer, 2003; Vurgaftman, Meyer, & Ram-Mohan, 2001). Hovel and Cuomo (Hovel & Cuomo, 1972) grew the first reported films of InN in 1972. Research onto InN was sporadic between 1938 and 1990, then the improved-quality InN was grown by plasma assisted molecular beam epitaxy (PA-MBE) in 1999 (Mamutin et al., 1999) but the turning point of the optical properties in this material happened when it was found that the apparent band gap energy for InN is near ~0.67 eV (Davydov et al., 2002a; Inushima et al., 2001), confirmation of this lower value has come through optical absorption and photo modulated reflectance measurements (Wu et al., 2002a) which is much smaller than the accepted value before 2001 where the band gap energy for InN was 1.9 eV, as determined by Tansley and Foley (Tansley & Foley, 1986). However, the recent determination of the band gap energy of wurtzite InN, as low as 0.7 eV, has opened a new field, extending the range of operation of III-nitrides into the near-infrared region of the electromagnetic spectrum.

For first-order Raman scattering and polarized infrared (IR) reflectance spectroscopy spectra with the theoretical calculation have been studied for hexagonal InN. The phonon frequencies at the center of the BZ found in the literatures are shown in Table 2.3.

Table 2.3: Phonon modes in wurtzite InN

Phonon modes	**Experimental (cm^{-1})**	**Theoretical (cm^{-1})**
E_2 (low)	87[a] , 87[b], ---	83[d],85[e]
E_2 (high)	488[a], 488[b], ---	483[d], 485[e]
E_1(LO)	593[a], 570[b], 574[c]	595[d], 596[e]
E_1(TO)	476[a], 476[b], 475[c]	467[d], 457[e]
A_1(LO)	586[a], 580[b], 574[c]	586[d], 587[e]
A_1(TO)	447[a], 480[b], 446[c]	443[d], 449[e]

[a] Taken from (Davydov et al., 1999);
[b] Taken from (Inushima, Shiraishi, & Davydov, 1999);
[c] Taken from (Dyck et al., 1999);
[d] Taken from (Bungaro, Rapcewicz, & Bernholc, 2000);
[e] Taken from (Tütüncü, Srivastava, & Duman, 2002).

2.3 Overview on the ternary compound semiconductor

Recently, many papers have appeared on the III-nitride ternary semiconductors. A large fraction of these papers is focused on the device applications and studies of the fundamental material properties. At present, the review in these subsections will be concerning on the most important properties of III-nitride ternary alloys, which includes difficulty in the materials growth with applications, band gap energy, band gap energy bowing parameter, and the behavior of the BZ optical phonon modes.

2.3.1 Wurtzite $Al_xGa_{1-x}N$

By varying the Al concentration in the $Al_xGa_{1-x}N$ ternary alloys ($0 \leq x \leq 1$), the direct energy band gap is tunable from 3.4 eV (360 nm in GaN) to 6.2 eV (200 nm in AlN). As a consequent, new applications are emerging for AlGaN based devices such as optoelectronic devices, UV photodetectors as well as application for sensor devices, particularly, operating under harsh environment conditions (Munoz et al., 2001).

The materials growth is wide and complicated. Therefore, in this review we will only describe the basics information of the growth difficulties for this ternary material which will add to the nitrides growth difficulties as mentioned in Chapter 1.

High-quality AlGaN films are the key element in obtaining efficient UV photo-detectors and light emitters. The growth of AlGaN has proven to be significantly difficult due to aluminium adatoms have a much larger sticking coefficient and much lower surface mobility than gallium adatoms. The layer-by-layer growth of films with attachment of adatoms at steps or kinks gives the smoothest surface features, as opposed to three-dimensional island growth. Because Al adatoms are much less mobile on the surface, they are unable to move from their point of impact on the surface from the vapor to energetically favourable lattice steps, resulting in three dimensional island growth. As a result, a high density of extended defects, such as dislocations and grain boundaries, are generated as the growth islands from different nucleation sites coalesce (Khan, Balakrishnan, & Katona, 2008; Khan et al., 2005).

Energy band gap is one of the most important parameters that characterize a semiconductor and determine many gross electronic and optical properties of the material, especially, the III-nitrides, having a wide direct band gap, to cover a broad spectral range from infrared to deep UV. The high energy bonds in these materials provide a high thermal stability and capability to withstand chemical aggressive and corrosive environments. A critical parameter to determine the alloy band gap energies is the band gap bowing parameter, which is a measure of nonlinearity of the energy gap functional dependence on composition. More details regarding band gap bowing parameter will be given in Chapter 3.

The band gap bowing parameter of the $Al_xGa_{1-x}N$ alloy as a function of Al composition x was reported by different authors to bend upward, downward, and also remain linear. The first reliable optical measurements of the alloy epilayer measurements were made by Koide et al. (Koide et al., 1987). The layers were grown by MOVPE on (0001) sapphire substrates with a 50 nm thick AlN buffer layer. A value of 1.060 eV was found for the bowing parameter b, which observed that the band gap of the alloy deviates downward showing a positive value for the bowing parameter. Also some researchers agreed to the positive bowing parameter b such as Lee et al. (Lee et al., 1999) that found the value $b = 0.62 \pm 0.45$ eV. Steude et al. (Steude et al., 1999) obtained $b = 0.6$ eV.

For theoretical simulations, the $Al_xGa_{1-x}N$ ternary bowing parameter value was $b = 0.353$ eV (Kuo & Lin, 2002). Also Suzuki et al. (Suzuki et al., 2000) reported a parabolic composition dependence of the $Al_xGa_{1-x}N$ fundamental band-gap energy with a positive bowing parameter of about 1.1 eV for $0 < x < 1.9$. While Yoshida et al. (Yoshida, Misawa, & Gonda, 1983b) concluded that, as the AlN mole fraction increases, the energy band gap of $Al_xGa_{1-x}N$ deviates upward, implying a negative value for the bowing parameter b. Another group investigated that there is no value of the bowing parameter ($b = 0$ eV) (Duda et al., 1998; Ochalski et al., 1999; Wickenden et al., 1994).

Angerer et al. (Angerer et al., 1997) have used $Al_xGa_{1-x}N$ epilayers grown with the plasma-induced MBE. They covered the whole composition range of the alloy from $0 \leq x \leq 1$. They also determined the lattice constants and showed that Vegard's law is valid for this alloy to a good approximation. A value of 1.3 eV of the bowing parameter was determined. Akasaki and Amano (Akasaki & Amano, 1998) have determined the band gaps of the strained $Al_xGa_{1-x}N$ layers using the PL method.

The bowing parameter was 0.25 eV for $Al_xGa_{1-x}N$ layers for values of x in the range $0 \leq x \leq 0.25$.

It is interesting to compare the values of the bowing parameters for different researchers. Considering the band gap difference between the end-point binary nitrides, values from 1 eV (Koide et al., 1987; Vurgaftman, Meyer, & Ram-Mohan, 2001) to 1.3 eV (Brunner et al., 1997) and on to 1.33 eV (Shan et al., 1999) have been reported in the literatures for the band gap bowing parameter of the AlGaN system. Finally, the overall discrepancy in the reported bowing parameters ranges from -0.8 eV (upward bowing) to 2.6 eV (downward bowing), as compiled by Yun et al. (Yun et al., 2002).

With respect to the phonon modes in hexagonal $Al_xGa_{1-x}N$, some group reported phonon data based on Raman scattering and IR absorption such as Hayashi et al. (Hayashi et al., 1991), Behr et al. (Behr et al., 1997a), Bergman et al. (Bergman et al., 1997), Demangeot et al. (Demangeot et al., 1997), Cros et al. (Cros et al., 1997a; Cros et al., 1997b), which seem to show that the frequencies of both the A_1 and E_1 polar Raman modes increase smoothly and continuously with increasing x, showing an one-mode behavior. Nevertheless, the experimental results are not all consistent with each other regarding the E_2 mode, which is probably attributable to significant differences in the quality of the samples used by different researchers.

A comprehensive study based on Raman scattering was reported by Davydov et al. (Davydov et al., 2002c). The authors used a large set of samples, including 2-4μm thick films with $0 < x < 0.5$ grown on sapphire, and 1-4 μm thick films with $0.5 < x < 1$ grown on Si (111). Both the A_1(LO) and E_1(LO) modes showed one-mode behavior, while the others, A_1(TO), E_1(TO), E_2(H) and E_2(L), showed two-mode behavior.

2.3.2 Wurtzite $In_xGa_{1-x}N$

The ternary semiconductor compound InGaN is one suitable candidate as the active layer in the violet, blue and green based light emitting diodes (LEDs) and laser diodes (LDs) because its band gap covered these spectral regions which depend on the indium mole fraction used. Several fundamental difficulties prevent the progress of the epitaxial growth technology of InGaN. The large difference in inter-atomic spacing between GaN and InN (lattice mismatch of 11%) makes the growth of InGaN alloys challenging, as it leads to compositional inhomogeneity and strains that strongly affect the optical properties of the InGaN layers. The growth at a high temperature of about 800 °C typically results in high crystalline quality but with low amount of InN incorporation because of the high equilibrium vapor pressure of nitrogen over InN. At the standard growth temperatures of GaN ~750 °C, the volatility of nitrogen over InN is more than ten orders of magnitude greater than that over GaN, therefore, the growth temperature of InGaN alloys is generally low to prevent dissociation (Doppalapudi, Basu, & Moustakas, 1999; Matsuoka, Sasaki, & Katsui, 1990). In addition, low miscibility of InN in GaN which leads to phase separation has been theoretically predicted and experimentally observed in InGaN with indium greater than 35% (Doppalapudi et al., 1998). Indium segregation is also a problem for InGaN films with high indium content. Attempts to increase the InN incorporation in the solid by raising the indium pressure in the vapor results in indium droplets formation (Shimizu, Hiramatsu, & Sawaki, 1994). Thus, the growth of high quality and In-rich InGaN films with good structural and optical properties depended sensitively on the growth temperature, V/III ratio (Bottcher et al., 1998; Kushi et al., 1999; Matsuoka, 1992), and the nitrogen flow rate (Komaki et al., 2007).

The fundamental band gap of the group III nitride InGaN ternary alloy system covers a wide spectral region ranging from the near infrared at ~1770 nm (0.7 eV for InN) to the ultraviolet at ~360 nm (3.4 eV for GaN). Since the energy gap for InN is smaller than that of GaN, the energy gap of the InGaN alloy decreases with increasing indium concentration. For the bandgap of $In_xGa_{1-x}N$, it appears that $In_xGa_{1-x}N$ alloy's bowing parameter is a strong function of In composition x and it decreases with increasing x (Parker et al., 1999). Based on some results from different groups, a summarized review regarding the energy bandgap bowing parameter is as follows.

Davydov et al. (Davydov et al., 2002b) described optical investigations of In-rich $In_xGa_{1-x}N$ alloy layers which have shown that the bowing parameter b~ 2.5 eV was found over the specific composition region ($0.36 < x < 1$).

McCluskey et al. (McCluskey et al., 1998) found that when the In content was less than 0.12 the bowing parameter will become as large as 3.5 eV, also Androulidaki et al. (Androulidaki et al., 2006) got the same value of bowing parameter 3.5 eV for $In_xGa_{1-x}N$ alloy at the whole composition range ($0 \leq x \leq 1$). In addition, many research groups obtained the bowing parameter for the InGaN and found that it was also large ranging from 2.4 eV to 4.5 eV (Aumer et al., 1999; Naranjo et al., 2002a; Naranjo et al., 2002b; Parker et al., 1999; Ryan et al., 2002; Schrenk et al., 1999; Siozade et al., 2000; Wetzel et al., 1998). While some academics researcher have suggested a relatively smaller value of bowing parameter as 1.4 eV (Wu et al., 2002b), 1.5 eV (Miyajima et al., 2002) and 1.6 eV (Ferhat, Furthmüller, & Bechstedt, 2002).

Some researcher got the bowing parameter for ternary $In_xGa_{1-x}N$ from theoretical simulation and found that the value b = 1.21 eV (Kuo, Lin, & Lin, 2001).